PHYSICAL REVIEW A VOLUME 37, NUMBER 1 JANUARY 1, 1988

Electron capture by fast protons from helium, nitrogen, and oxygen: The corrected first Born approximation

Dževad Belkić
Institute of Physics, Post Office Box 57, 11001, Belgrade, Yugoslavia

(Received 29 June 1987)

The first Born approximation corrected for the boundary conditions is used to compute total cross sections for charge exchange in H^+-He, H^+-N, and H^+-O collisions at intermediate and high energies. An independent-particle method is employed with a one-electron orbital for the target. Two sets of computation are presented in which the initial state of the active electron is described by the Roothaan-Hartree-Fock and hydrogenlike wave functions. These two approaches yield noticeably different results for the cross sections. Excellent agreement with existing experimental data is obtained at energies ranging from 50 keV to 50 MeV by using the Roothaan-Hartree-Fock wave function as a linear combination of normalized Slater-type orbitals.

I. INTRODUCTION

Charge exchange in collisions between bare projectiles and multielectron atoms has been the subject of many experiments over the years. The most numerous are the early measurements on total capture which could not isolate any specific shell of the target.[1–5] At low energies, the dominant contribution to total capture is provided by electrons from the outermost target shells. The situation is reversed at high energies, where the inner-shell electrons yield the most significant fraction of the total capture. In the intermediate-energy region, inner- and outer-shell capture are of equal importance. Interference between these two contributions is responsible for an appreciable change in the curvature in the total cross sections.[2,5,6] This is in contrast to the collision of bare nuclei with genuine single-electron atoms, for which the cross sections relating to a given target state vary monotonically at all energies.[6]

Capture from an inner shell of complex atoms is experimentally difficult to isolate and the available data are scarce.[7–11] Multiple scatterings preclude the coincident detection of charge exchange and K-vacancy production for large values of the projectile nuclear charge Z_P. Nevertheless, in this case, electron transfer from the K shell of multielectron targets to the ground state of the hydrogenlike atom can indirectly be determined. This has customarily been done by subtracting the Z_P^2-scaled ionization cross sections from experimental data on the K-shell vacancy production.[9,12] At lower Z_P, however, multiple processes are less effective and the measurement becomes feasible. The coincident detection of newly formed hydrogenic atoms and Auger electron signals provides the ratio of the cross sections for capture and total vacancy production from an inner shell of the target. These recently measured ratios,[7–10] together with the earlier recorded data for the total inner-shell vacancy production, have been used to extract pure electron-capture cross sections for a specific inner shell of multielectron atoms.[12–16]

An interest in electron capture by ionized projectiles from multielectron atoms arose with regard to the production of inner-shell vacancies. It is now well established that the deviation from the Z_P^2-charge dependence of the total inner-shell vacancy production can be accounted for by inclusion of a charge-exchange channel.[9,12,17] Electron transfer is also crucial in thermonuclear fusion devices using neutral beam injection heating and refueling of magnetically confined plasmas.[18–21] Processes employing atomic oxygen to produce x-ray lines involve charge exchange between low-energy cosmic rays and interstellar gases.[22,23]

Recent experimental data on electron capture from a particular inner shell of multielectron atoms at high energies[7–11] have prompted much theoretical work.[6,24–28] Computations based upon inclusion of electron correlation effects in perturbation potentials and wave functions are not yet available. However, this seems to be unnecessary since a wide separation of binding energies for the inner-shell electrons of heavy targets justifies the use of an independent-particle model.[29] In this approach, all the target electrons interact independently with the projectile, and the transition probability for a given electron is unaltered by the presence of the remaining electronic core.[30] These nonparticipating, passive electrons merely screen the target nuclear charge seen by the projectile and the active electron. The screening has most frequently been introduced by considering the Coulomb potential with an effective charge accompanied by the hydrogenlike wave function for the target.[24–26] The binding energy of the active electron was subsequently chosen from the experimentally determined ionization potentials. The rationale for this was the substantial difference between the hydrogenic energy and the actual inner-shell binding energy.[31] However, elimination of this energy deviation has been achieved independently of the effective charge selection. Hence, the additional problem of the "post-prior" discrepancy arose despite the use of exactly known hydrogenic orbitals.

Previous theoretical studies, with the exception of Refs. 6 and 28, have ignored the boundary conditions which account for the correct asymptotic behaviors of the scattering wave functions at large interaggregate separations. The asymptotic convergence problem, treated in an *exact* theory, becomes irrelevant for protons incident on neutral multielectron targets.[32] However, in practice, resorting to approximate descriptions becomes inevitable and neutral heavy atoms are usually treated as one-electron systems with an effective nuclear charge. Such a model is, however, no longer free from the asymptotic Coulomb interactions between the colliding particles. Therefore, the unperturbed channel scattering states must exhibit distortions even when protons are used as projectiles. Hence, the Coulomb wave functions, or equivalently, their eikonal phase factors, should be employed instead of the plane waves for the relative motion of heavy particles. This departure from plane waves has often been assumed to be "minimal," but this assumption has not been substantiated. On the contrary, it has recently been demonstrated within the first Born approximation that the boundary conditions are essential for charge exchange.[33–37] In particular, the sole introduction of the Coulomb phase into the exit channel within the Jackson-Schiff (JS) matrix element for H^+-Ar charge exchange reduced the calculated cross sections by about 200 times, so that the first-order theory and experiment are now in agreement.[34]

In the present paper a first-order theory is formulated for charge exchange between completely stripped projectiles and arbitrary multielectron atoms. The usual first Born approximation is corrected for the boundary conditions in both entrance and exit channels [hereafter called corrected first Born (CB1) approximation]. In general, these corrections refer to (i) the Coulomb distortion of the unperturbed channel states and (ii) the perturbing potentials. The two modifications are consistent with each other. Hydrogenic and Roothaan-Hartree-Fock (RHF) models are investigated by approximating the nonlocal atom potentials with an effective Coulomb interaction. In both of these independent-particle methods the effective charge of the target nucleus is chosen in such a way that the hydrogenic energy relation is satisfied, i.e., $Z_T^{\text{eff}}=(-2E_i^{\text{RHF}})^{1/2}n^i$, where E_i^{RHF} is the RHF orbital energy and n^i is the principal quantum number of the orbital occupied by the active electron. In this way the present model with the hydrogenlike wave functions does not exhibit the post-prior discrepancy. The RHF orbital energy E_i^{RHF}, which is computed by means of a self-consistent-field (SCF) technique,[38] is known to be in close agreement with the experimental binding energies. In the RHF model, the initial target state is described by a linear combination of the normalized Slater-type orbitals (STO) with the parameters obtained by Clementi and Roetti.[38] Such a wave function is not exact and, therefore, the "post" (T_{if}^+) and the "prior" (T_{if}^-) transition amplitudes are unequal. The post-prior discrepancy can be avoided by introducing a new transition amplitude as an arithmetic average of T_{if}^+ and T_{if}^-. This procedure is adopted in the present work, which reports the results of detailed computations on charge exchange in H^+-He, H^+-N, and H^+-O collisions at intermediate and high energies.

II. THEORY

Consider a rearrangement scattering in which a bare nucleus of charge Z_P impinges upon an arbitrary multielectron atom or ion $X_i^{(q)+}$, i.e. (atomic units will be used throughout unless otherwise stated),

$$Z_P+X_i^{(q)+}\rightarrow(Z_P,e)_f+X_{i'}^{(q+1)+} \ . \tag{2.1}$$

The target of charge state q possesses $N+1$ electrons in the initial state (i). The electronic state of the hydrogenlike bound system $(Z_P,e)_f$ is described by the usual set of quantum numbers $n^f l^f m^f \equiv f$. A simple model for process (2.1) has been proposed by Belkić *et al.*[6] and was subsequently implemented by Belkić and Taylor[35] in the first Born approximation with correct boundary conditions (CB1). In this model the set of N noncaptured electrons is considered to be "passive," such that their interactions with the active electron e do not contribute to the capture process. It is also assumed that these passive electrons occupy the same orbitals before and after the collision. As a consequence of such a simplification, an explicit introduction of N passive electrons into the T matrix for reaction (2.1) is avoided. Furthermore, it is taken that the perturbing potentials V_i and V_f in the entrance and exit channel contain only Coulomb interactions. In this way the pure three-body nature of the rearrangement collision is preserved. It is within this model that we impose the correct boundary conditions to the scattering wave functions. Then we can introduce the appropriate prior and post forms of the transition amplitude for process (2.1) as follows:

$$T_{if}^-(\eta)=\int\int d\mathbf{R}\,d\mathbf{r}_T\Phi_f^{-*}V_i\Phi_i^+ \ , \tag{2.2a}$$

$$T_{if}^+(\eta)=\int\int d\mathbf{R}\,d\mathbf{r}_P\Phi_f^{-*}V_f\Phi_i^+ \ , \tag{2.2b}$$

where η is the transverse momentum transfer, and

$$V_i=\frac{Z_P}{R}-\frac{Z_P}{r_P}, \quad V_f=\frac{Z_T^{\text{eff}}}{R}-\frac{Z_T^{\text{eff}}}{r_T} \ , \tag{2.3}$$

$$\Phi_i^+=\varphi_i^{\text{RHF}}(\mathbf{r}_T)\exp\left[i\mathbf{k}_i\cdot\mathbf{r}_i+\frac{Z_P(Z_T^{\text{eff}}-1)}{v}\ln(vR-\mathbf{v}\cdot\mathbf{R})\right]\equiv\Phi_i\exp\left[i\frac{Z_P(Z_T^{\text{eff}}-1)}{v}\ln(vR-\mathbf{v}\cdot\mathbf{R})\right] , \tag{2.4a}$$

$$\Phi_f^-=\varphi_f^{Z_P}(\mathbf{r}_P)\exp\left[-i\mathbf{k}_f\cdot\mathbf{r}_f-i\frac{Z_T^{\text{eff}}(Z_P-1)}{v}\ln(vR+\mathbf{v}\cdot\mathbf{R})\right]\equiv\Phi_f\exp\left[-i\frac{Z_T^{\text{eff}}(Z_P-1)}{v}\ln(vR+\mathbf{v}\cdot\mathbf{R})\right] . \tag{2.4b}$$

Here $\mathbf{v}$ is the incident velocity vector, $\mathbf{k}_i$ and $\mathbf{k}_f$ are the initial and final wave vectors, $\mathbf{R}$ is the relative vector of the target nucleus with respect to the projectile, and $\mathbf{r}_P$ and $\mathbf{r}_T$ are the vectors of the active electron relative to the projectile and target nucleus. Functions $\varphi_i^{\mathrm{RHF}}(\mathbf{r}_T)$ and $\varphi_f^{Z_P}(\mathbf{r}_P)$ are the orbitals of the active electron in the initial and final state, respectively. Furthermore, in the usual eikonal mass limit, we shall have

$$\mathbf{k}_i\cdot\mathbf{r}_i+\mathbf{k}_f\cdot\mathbf{r}_f=-\mathbf{v}\cdot\mathbf{r}_T-\boldsymbol{\alpha}\cdot\mathbf{R}\ , \tag{2.5a}$$

$$=-\mathbf{v}\cdot\mathbf{r}_P+\boldsymbol{\beta}\cdot\mathbf{R}\ , \tag{2.5b}$$

where

$$\boldsymbol{\eta}=(\eta\cos\phi_\eta,\eta\sin\phi_\eta,0)$$

and

$$\boldsymbol{\alpha}=\alpha_z\hat{\mathbf{v}}+\boldsymbol{\eta};\quad \alpha_z=-v/2+\Delta E/v\ , \tag{2.6a}$$

$$\boldsymbol{\beta}=\beta_z\hat{\mathbf{v}}-\boldsymbol{\eta};\quad \beta_z=-v/2-\Delta E/v\ , \tag{2.6b}$$

$$\Delta E=E_i^{\mathrm{RHF}}-E_f;\quad E_f=-(Z_P/n^f)^2/2\equiv -a_f^2/2\ . \tag{2.6c}$$

Capture process (2.1) can, at least formally, be compared with the pure three-body problem of the type

$$Z_P+(Z_T,e)_i\to(Z_P,e)_f+Z_T\ , \tag{2.7}$$

where Z_T is the target nuclear charge. In this case there is no post-prior discrepancy and the transition amplitude can be calculated from either of the two following matrix elements:

$$T_{if}^-(\boldsymbol{\eta})=\int\int d\mathbf{R}\,d\mathbf{r}_T\varphi_f^{Z_P*}(\mathbf{r}_P)\left[\frac{Z_P}{R}-\frac{Z_P}{r_P}\right]\varphi_i^{Z_T}(\mathbf{r}_T)\times\exp(i\mathbf{k}_i\cdot\mathbf{r}_i+i\mathbf{k}_f\cdot\mathbf{r}_f)\mathscr{E}(\mathbf{R})\ , \tag{2.8a}$$

$$T_{if}^+(\boldsymbol{\eta})=\int\int d\mathbf{R}\,d\mathbf{r}_P\varphi_f^{Z_P*}(\mathbf{r}_P)\left[\frac{Z_T}{R}-\frac{Z_T}{r_T}\right]\varphi_i^{Z_T}(\mathbf{r}_T)\times\exp(i\mathbf{k}_i\cdot\mathbf{r}_i+i\mathbf{k}_f\cdot\mathbf{r}_f)\mathscr{E}(\mathbf{R})\ , \tag{2.8b}$$

$$\mathscr{E}(\mathbf{R})=\exp\left[i\frac{Z_P(Z_T-1)}{v}\ln(vR-\mathbf{v}\cdot\mathbf{R})+i\frac{Z_T(Z_P-1)}{v}\ln(vR+\mathbf{v}\cdot\mathbf{R})\right]\ , \tag{2.8c}$$

where $\varphi_i^{Z_T}(\mathbf{r}_T)$ is the hydrogenlike wave function for the target system $(Z_T,e)_i$. It then follows that Eqs. (2.2) and (2.8) differ from each other in three important aspects: (i) the introduction of an effective charge Z_T^{eff} in place of Z_T, (ii) the appearance of the RHF wave function for the target instead of the hydrogenlike bound state, and (iii) the replacement of the hydrogenic energy $E_i=-(Z_T/n^i)^2/2$ by the appropriate RHF orbital energy E_i^{RHF}. As we have already emphasized, the present theory requires that the three-body nature of charge exchange for process (2.1) be preserved. This has alleviated an explicit introduction of the dynamic of N passive electrons into the transition amplitudes (2.2a) and (2.2b). Nevertheless, these passive electrons are implicitly present in the SCF technique used to compute both the RHF wave function for the multielectron target $X_i^{(q)+}$ and the associated RHF orbital energy E_i^{RHF}. Hence, the present theory for process (2.1) represents a substantial improvement over the customary hydrogenic model.[24–26] In this latter model, the methods available for process (2.7) have been extended to reaction (2.1) in a straightforward manner by simply using certain Z_T^{eff} instead of Z_T and by employing the pure hydrogenic wave function for the initial state of the multielectron target.[24–26] Moreover, such a hydrogenic model violates its own boundary conditions for process (2.1) in the same fashion as has customarily been done for reaction (2.7).

We shall presently choose an analytical form of the RHF wave function which has been obtained by Clementi and Roetti[38] with the help of the SCF technique, i.e.,

$$\varphi_i^{\mathrm{RHF}}(\mathbf{r}_T)\equiv\varphi_{n^il^im^i}^{\mathrm{RHF}}(\mathbf{r}_T)=\sum_{k=1}^{N_i}c_k\chi_{n^{(k)}l^im^i}^{(\lambda_k)}(\mathbf{r}_T)\ . \tag{2.9a}$$

Here, c's are the coefficients associated with the normalized STO's $\chi_{n^{(k)}l^im^i}^{(\lambda_k)}(\mathbf{r}_T)$,

$$\chi_{n^{(k)}l^im^i}^{(\lambda_k)}(\mathbf{r}_T)=N_k^{\lambda_k}r_T^{n^{(k)}-1}e^{-\lambda_kr_T}Y_{l^im^i}(\hat{\mathbf{r}}_T)\ , \tag{2.9b}$$

where $Y_{l^im^i}(\hat{\mathbf{r}}_T)$ is the usual spherical harmonic, $n^{(k)}$ is the orbital number, and λ's are variational parameters,

$$N_k^{\lambda_k}=[(2\lambda_k)^{1+2n^{(k)}}/(2n^{(k)})!]^{1/2}\ . \tag{2.10}$$

Upper summation index N_i in Eq. (2.9a) represents the total number of the STO's used in describing a given shell of the target from which capture is taking place. Parameters c_k, λ_k, E_i^{RHF}, and N_i are given in a tabular form in Ref. 38. In the present study, we shall choose the following value for the effective charge Z_T^{eff}, as suggested by Belkić *et al.*:[6]

$$Z_T^{\mathrm{eff}}=n^i(-2E_i^{\mathrm{RHF}})^{1/2}\ , \tag{2.11}$$

where n^i is the principal quantum number of the target initial orbital from which the active electron is transferred to the projectile.

Setting $\mathbf{R}=\boldsymbol{\rho}+\mathbf{Z}$, where

$$\hat{\boldsymbol{\rho}}=(\cos\phi_\eta,\sin\phi_\eta,0)\ ,$$

and $Z=\mathbf{R}\cdot\hat{\mathbf{v}}$, we shall have

$$T_{if}^-(\boldsymbol{\eta})=\int\int d\mathbf{R}\,d\mathbf{r}_T(\rho v)^{2i\nu_\beta}\Phi_f^*V_i\Phi_i(vR+\mathbf{v}\cdot\mathbf{R})^{-i\xi}\ , \tag{2.12a}$$

$$T_{if}^+(\boldsymbol{\eta})=\int\int d\mathbf{R}\,d\mathbf{r}_P(\rho v)^{2i\nu_\beta}\Phi_f^*V_f\Phi_i(vR+\mathbf{v}\cdot\mathbf{R})^{-i\xi}\ , \tag{2.12b}$$

with $\nu_\beta=Z_P(Z_T^{\mathrm{eff}}-1)/v$ and $\xi=(Z_T^{\mathrm{eff}}-Z_P)/v$. Transition amplitude (2.12a) yields different cross sections from those obtained by means of Eq. (2.12b), and it is advantageous to eliminate this post-prior discrepancy. Hence, the following symmetric form of the arithmetic average transition amplitude will be used in the present computation (see also Ref. 35):

$$T_{if}(\boldsymbol{\eta})=\tfrac{1}{2}[T_{if}^{-}(\boldsymbol{\eta})+T_{if}^{+}(\boldsymbol{\eta})] \ . \tag{2.13}$$

The total cross section for process (2.1) is introduced by

$$\begin{aligned}\sigma_{if}(a_0^2)&=n_0\int d\boldsymbol{\eta}\left|\frac{T_{if}(\boldsymbol{\eta})}{2\pi v}\right|^2\\&=n_0\int_0^{\infty}d\eta\,\eta\int_0^{2\pi}d\phi_\eta\left|\frac{T_{if}(\boldsymbol{\eta})}{2\pi v}\right|^2 ,\end{aligned}\tag{2.14}$$

where n_0 is the number of electrons in the target shell from which the capture is occurring. We shall be concerned with a nonrelativistic approximation in which the target electrons are treated as distinguishable. Computations will be carried out for capture of one electron. Within the nonrelativistic theory, the total cross section is multiplied by the number of electrons in the active orbital. This is because each of the electrons occupying the active target orbital can be captured with equal probability. Inserting Eqs. (2.12a), (2.12b), and (2.13) into Eq. (2.14), it is readily verified that

$$\sigma_{if}(a_0^2)=n_0\int d\boldsymbol{\eta}\left|\frac{T_{if}(\boldsymbol{\eta})}{2\pi v}\right|^2 , \tag{2.15a}$$

$$\sigma_{if}(a_0^2)=n_0\int d\boldsymbol{\rho}\left|\frac{\mathcal{A}_{if}(\boldsymbol{\rho})}{2\pi v}\right|^2 , \tag{2.15b}$$

$$\sigma_{if}(a_0^2)=n_0\int d\boldsymbol{\eta}\left|\frac{\mathcal{J}_{if}(\boldsymbol{\eta})}{2\pi v}\right|^2 , \tag{2.15c}$$

where

$$\begin{aligned}\mathcal{A}_{if}(\boldsymbol{\rho})=\tfrac{1}{2}\int\int d\boldsymbol{\rho}\,dZ\,\varphi_f^{Z_P*}(\mathbf{r}_p)(V_i+V_f)\varphi_i^{\mathrm{RHF}}(\mathbf{r}_T)\\ \times(\rho v)^{2i\nu_\beta}(vR+\mathbf{v}\cdot\mathbf{R})^{-i\xi}\\ \times\exp\left[-i\mathbf{v}\cdot\mathbf{r}-i\frac{\Delta E}{v}Z\right] ,\end{aligned}\tag{2.16a}$$

$$\mathcal{J}_{if}(\boldsymbol{\eta})=\tfrac{1}{2}[\mathcal{J}_{if}^{-}(\boldsymbol{\eta})+\mathcal{J}_{if}^{+}(\boldsymbol{\eta})] , \tag{2.16b}$$

$$\mathcal{J}_{if}^{\pm}(\boldsymbol{\eta})=\int\int d\mathbf{R}\,d\mathbf{r}_T\Phi_f^*V_{f,i}\Phi_i(vR+\mathbf{v}\cdot\mathbf{R})^{-i\xi} , \tag{2.16c}$$

and $\mathbf{r}=(\mathbf{r}_P+\mathbf{r}_T)/2$.

Thus, it follows from Eqs. (2.15a) and (2.15c) that the term $(\rho v)^{2i\nu_\beta}$ can be omitted from transition amplitudes (2.12a) and (2.12b) in the computation of the total cross sections. This enormously simplifies the evaluation of matrix elements.

III. CALCULATION OF MATRIX ELEMENTS

Introducing the Fourier transform $\tilde{f}(\mathbf{q})$ by

$$\tilde{f}(\mathbf{q})=(2\pi)^{-3}\int d\mathbf{r}\,e^{i\mathbf{q}\cdot\mathbf{r}}f(\mathbf{r}) , \tag{3.1}$$

we obtain

$$\mathcal{J}_{if}^{-}(\boldsymbol{\eta})=Z_P I_{if,0}^{(1,0)}(\boldsymbol{\eta})-\tfrac{1}{2}I_{if,1}^{(1,-1)}(\boldsymbol{\eta}) , \tag{3.2}$$

$$\mathcal{J}_{if}^{+}(\boldsymbol{\eta})=Z_T^{\mathrm{eff}}I_{if,0}^{(1,0)}(\boldsymbol{\eta})-Z_T^{\mathrm{eff}}I_{if,1}^{(0,0)}(\boldsymbol{\eta}) , \tag{3.3}$$

where

$$I_{if,\sigma}^{(\nu_i,\nu_f)}(\boldsymbol{\eta})=(2\pi)^3\int d\mathbf{R}\,R^{\sigma-1}(vR+\mathbf{v}\cdot\mathbf{R})^{-i\xi}\int d\mathbf{q}\,e^{-i\mathbf{q}\cdot\mathbf{R}}\frac{\tilde{\varphi}_f^{Z_P*}(\mathbf{q}-\boldsymbol{\alpha})\tilde{\psi}_i^{(\nu_i)}(\mathbf{q}+\boldsymbol{\beta})}{(|\mathbf{q}-\boldsymbol{\alpha}|^2+a_f^2)^{\nu_f}} , \tag{3.4}$$

and

$$\begin{aligned}\psi_i^{(\nu_i)}(\mathbf{r}_T)&=r_T^{\nu_i-1}\varphi_i^{\mathrm{RHF}}(\mathbf{r}_T) , &(3.5\mathrm{a})\\&=\sum_{k=1}^{N_i}c_k r_T^{\nu_i-1}\chi_{n^{(k)}l^i m^i}^{(\lambda_k)}(\mathbf{r}_T)\\&\equiv\sum_{k=1}^{N_i}c_k\chi_{n^{(k)}l^i m^i}^{(\lambda_k,\nu_i)}(\mathbf{r}_T) . &(3.5\mathrm{b})\end{aligned}$$

Normalized STO's in momentum space $\tilde{\chi}_{n^{(k)}l^i m^i}^{(\lambda_k)}(\mathbf{q})$ can be expressed in terms of the Gegenbauer polynomials and spherical harmonics (Belkić[39]). The most convenient representation of these Fourier transforms, which is required for the calculation of integral (3.4), is the power-series representation. Thus, using formula (22.3.4) of Abramowitz and Stegun,[40] we deduce

$$\tilde{\psi}_{n^i l^i m^i}^{(\nu_i)}(\mathbf{q})=\sum_{k=1}^{N_i}c_k\tilde{\chi}_{n^{(k)}l^i m^i}^{(\lambda_k,\nu_i)}(\mathbf{q}) , \tag{3.6}$$

$$\begin{aligned}\tilde{\chi}_{n^i l^i m^i}^{(\lambda_k,\nu_i)}(\mathbf{q})=\frac{(2i)^{l^i}}{2\pi^2}(n_r^k+\nu_i)!l^i!N_k^{\lambda_k}\\ \times\frac{C_{n_r^k+\nu_i}^{l^i+1}(\lambda_k/\sqrt{q^2+\lambda_k^2})}{(q^2+\lambda_k^2)^{1+l^i+(n_r^k+\nu_i)/2}}\mathcal{Y}_{l^i m^i}(\mathbf{q}) ,\end{aligned}\tag{3.7}$$

$$=(2\pi)^{-3}\mathcal{N}_k^{\lambda_k}i^{l^i}\sum_{p_{i1}=0}^{(n_r^k+\nu_i)/2}c_{p_{i1}}\frac{\mathcal{Y}_{l^i m^i}(\mathbf{q})}{(q^2+\lambda_k^2)^{n_i+1}} , \tag{3.8}$$

$$\tilde{\varphi}_{n^f l^f m^f}^{Z_P}(\mathbf{q})=(2\pi)^{-3}N_f^{Z_P}i^{l^f}\sum_{p_f=0}^{n_r^f}c_{p_f}\frac{\mathcal{Y}_{l^f m^f}(\mathbf{q})}{(q^2+a_f^2)^{p_f+l^f+2}} , \tag{3.9}$$

where $\mathcal{Y}_{lm}(\mathbf{q})$ is the solid spherical harmonic and $[(n_r^k+\nu_i)/2]$ is the integral part of the fraction $(n_r^k+\nu_i)/2$. Further,

$$N_f^{Z_P}=\frac{16\pi Z_P[(a_f^3/n^f)(n^f+l^f)!]^{1/2}l^f!(4a_f)^{l^f}}{(2l^f+1)!}\ , \tag{3.10a}$$

$$\mathcal{N}_k^{\lambda_k}=16\pi(n_r^k+\nu_i)!2^{l^i-2}N_k^{\lambda_k}\ , \tag{3.10b}$$

$$c_{p_f}=\frac{(-n_r^f)_{p_f}(n^f+l^f+1)_{p_f}}{(l^f+3/2)_{p_f}p_f!}a_f^{2p_f}\ , \tag{3.10c}$$

$$c_{p_{i1}}=\frac{(-1)^{p_{i1}}(2\lambda_k)^{p'_{i2}+\nu_i}(p_{i2}+\nu_i-1)!}{p_{i1}!(p'_{i2}+\nu_i)!}\ , \tag{3.10d}$$

$$n_r^f=n^f-l^f-1,\quad n_r^k=n^{(k)}-l^i-1\ ,$$
$$(a)_n=\Gamma(a+n)/\Gamma(a)\ , \tag{3.10e}$$

$$p_{i1}+p_{i2}=n^{(k)},\quad p'_{i1}+p'_{i2}=n_r^k\ ,$$
$$p'_{i1}=2p_{i1},\quad n_i=p_{i2}+\nu_i-1\ . \tag{3.10f}$$

Auxiliary integral (3.4) can now be written in the following form:

$$I_{if}^{(\nu_i,\nu_f)}(\eta)=i^{l^i}(-i)^{l^f}N_f^{Z_P}\sum_{k=1}^{N_i}d_k\sum_{p_{i1}=0}^{[(n_r^k+\nu_i)/2]}c_{p_{i1}}\sum_{p_f=0}^{n_r^f}c_{p_f}H_{n_in_f;\sigma}^{(\nu_i,\nu_f)}(\boldsymbol{\alpha},\boldsymbol{\beta})\ , \tag{3.11}$$

where $d_k=c_k\mathcal{N}_k^{\lambda_k}$,

$$H_{n_in_f;\sigma}^{(\nu_i,\nu_f)}(\boldsymbol{\alpha},\boldsymbol{\beta})=2\pi^2\mathcal{H}_{n_in_f;\sigma}^{(\nu_i,\nu_f)}(\boldsymbol{\alpha},\boldsymbol{\beta})\ , \tag{3.12a}$$

$$\mathcal{H}_{n_in_f;\sigma}^{(\nu_i,\nu_f)}(\boldsymbol{\alpha},\boldsymbol{\beta})=(2\pi)^{-3}\int d\mathbf{R}\,R^{\sigma-1}(vR+\mathbf{v}\cdot\mathbf{R})^{-i\xi}\mathcal{G}_{n_in_f}^{\nu_i\nu_f}(-\mathbf{R})\ , \tag{3.12b}$$

$$\mathcal{G}_{n_in_f}^{\nu_i\nu_f}(\mathbf{R})=\frac{1}{2\pi^2}\int d\mathbf{q}\,e^{i\mathbf{q}\cdot\mathbf{R}}\frac{\mathcal{Y}^*_{l^fm^f}(\mathbf{q}-\boldsymbol{\alpha})\mathcal{Y}_{l^im^i}(\mathbf{q}+\boldsymbol{\beta})}{(|\mathbf{q}-\boldsymbol{\alpha}|^2+a_f^2)^{n_f+1}(|\mathbf{q}+\boldsymbol{\beta}|^2+\lambda_k^2)^{n_i+1}}\ , \tag{3.12c}$$

and

$$n_f=p_f+l^f+\nu_f+1\ . \tag{3.13}$$

The final result of integral (2.12a) is given by,[35]

$$\begin{aligned}H_{n_in_f;\sigma}^{(\nu_i,\nu_f)}(\boldsymbol{\alpha},\boldsymbol{\beta})=&\frac{1}{n_i!n_f!}\sum_{l_1^i=0}^{l^i}\sum_{l_1^f=0}^{l^f}\sum_{m_1^i=-l_1^i}^{+l_1^i}\sum_{m_1^f=-l_1^f}^{+l_1^f}\sum_{l=l^{if}}^{\lambda}{}^{(2)}(-1)^{(\lambda+l)/2}\frac{(2n_r)!}{n_r!}\Omega_{l_1^im_1^i}^{l_1^fm_1^f}(l,\mathbf{v})\\&\times\sum_{p=0}^{n_r}\frac{(-n_r)_p}{(-2n_r)_p}\,{}_3F_2\left[-n,-\lambda_l,-n_r+p;-n_r+\frac{p}{2},-n_r+\frac{p+1}{2};1\right]\frac{2^{p-2n_r-1}}{p!}\\&\times\int_0^1dt\,t^{n_f+l_2^i}(1-t)^{n_i+l_2^f}\frac{G_{\bar{p}lm}^{(\sigma,\Delta)}(\mathbf{Q},\mathbf{v})}{\Delta^{2n-(\lambda+l)-p-1}}\ ,\end{aligned} \tag{3.14}$$

where the upper index (2) in Eq. (3.14) associated with symbol $\sum^{(2)}$ indicates that the summation over l must be performed in steps of two (see Appendix). Here, we have

$$\mathbf{Q}=\boldsymbol{\alpha}t-\boldsymbol{\beta}(1-t),\quad \Delta^2=v^2t(1-t)+a_f^2t+\lambda_k^2(1-t),\quad \mathbf{v}=-\boldsymbol{\alpha}-\boldsymbol{\beta}\ ,$$

and

$$\Omega_{l_1^im_1^i}^{l_1^fm_1^f}(l,\mathbf{v})=(l_1^im_1^i\,|\,l^im^i)(l_1^fm_1^f\,|\,l^fm^f)\langle l_1^im_1^i\,|\,l_1^fm_1^f\,|\,lm\rangle\mathcal{Y}^*_{l_2^fm_2^f}(\mathbf{v})\mathcal{Y}_{l_2^im_2^i}(-\mathbf{v})\ , \tag{3.15a}$$

$$G_{\bar{p}lm}^{(\sigma,\Delta)}(\mathbf{Q},\mathbf{v})=\sum_{\kappa=0}^{p_\sigma}\sum_{l_1=0}^{l}\mathcal{J}_{pl}^{\kappa l_1}(\sigma)D_{lm}^{l_1}(\mathbf{Q},\mathbf{v})\ , \tag{3.15b}$$

$$\mathcal{J}_{pl}^{\kappa l_1}(\sigma)=ab\,{}_3F_2\left[-\frac{\kappa_\sigma}{2},-\frac{\kappa_\sigma-1}{2},1-i\gamma_1,\kappa+l+1,-p_\sigma-1;\frac{\Delta^2+Q^2}{\Delta^2}\right]\ , \tag{3.15c}$$

$$D_{lm}^{l_1}(\mathbf{Q},\mathbf{v})=\sum_{m_1=-l_1}^{+l_1}(l_1m_1\,|\,lm)\mathcal{Y}_{l_1m_1}(\mathbf{Q})\mathcal{Y}_{l_2m_2}(-i\mathbf{v})\ , \tag{3.15d}$$

where

$$(l_1^f m_1^f \mid l^f m^f) = \left[4\pi \frac{2l^f+1}{(2l_1^f+1)(2l_2^f+1)} \frac{(l^f+m^f)!}{(l_1^f+m_1^f)!(l_2^f+m_2^f)!} \frac{(l^f-m^f)!}{(l_1^f-m_1^f)!(l_2^f-m_2^f)!} \right]^{1/2} , \tag{3.16a}$$

$$(l_1 m_1 \mid lm) = \left[4\pi \frac{2l+1}{(2l_1+1)(2l_2+1)} \frac{(l+m)!}{(l_1+m_1)!(l_2+m_2)!} \frac{(l-m)!}{(l_1-m_1)!(l_2-m_2)!} \right]^{1/2} , \tag{3.16b}$$

$$\langle l_1^i m_1^i \mid l_1^f m_1^f \mid lm \rangle = (-1)^{m_1^i} \left[\frac{(2l_1^i+1)(2l_1^f+1)(2l+1)}{4\pi} \right]^{1/2} \begin{bmatrix} l_1^f & l_1^i & l \\ 0 & 0 & 0 \end{bmatrix} \begin{bmatrix} l_1^f & l_1^i & l \\ -m_1^f & m_1^i & -m \end{bmatrix} , \tag{3.16c}$$

$$a = \Gamma(1-i\xi)(l+1)_{p_\sigma} \frac{(2\Delta)^{p_\sigma}}{(\Delta^2+Q^2)^{p_\sigma+l+1}} , \tag{3.16d}$$

$$b = \frac{(1-i\xi)_{l_1}(i\xi)_{l_2}}{x^{i\gamma_2}} \frac{(-p_\sigma)_\kappa (i\gamma_2)_\kappa}{(l+1)_\kappa} \frac{(1-y/x)^\kappa}{\kappa!} , \tag{3.16e}$$

$$x = \frac{2}{Q^2+\Delta^2}(v\Delta - i\mathbf{Q}\cdot\mathbf{v}), \quad y = v/\Delta , \tag{3.16f}$$

and

$$l_1^j + l_2^j = l^j, \quad m_1^j + m_2^j = m^j, \quad -l_2^j \le m_2^j \le +l_2^j \quad (j = i,f); \quad m = m_1^f - m_1^i , \tag{3.17a}$$

$$l^{if} = \begin{cases} \max(|l_1^i - l_1^f|, |m|) & \text{if } \max(|l_1^i - l_1^f|, |m|) + \lambda \text{ even} \\ \max(|l_1^i - l_1^f|, |m|) + 1 & \text{if } \max(|l_1^i - l_1^f|, |m|) + \lambda \text{ odd} , \end{cases} \tag{3.17b}$$

$$\lambda = l_1^i + l_1^f, \quad l_1 + l_2 = l, \quad m_1 + m_2 = m ; \quad -l_2 \le m_2 \le +l_2 , \tag{3.17c}$$

$$n_r = n - l - 1, \quad n = n_i + n_f + 1; \quad \kappa_\sigma = p_\sigma - \kappa, \quad p_\sigma = p + \sigma , \tag{3.17d}$$

$$\gamma_1 = \xi + il_1, \quad \gamma_2 = \xi - il_2 . \tag{3.17e}$$

The Claussen generalized hypergeometrical polynomial ${}_3F_2$ occurring in Eqs. (3.14) and (3.15c) and defined

$${}_3F_2 \left[-n, -\lambda_l, -n_r+p; -n_r+\frac{p}{2}, -n_r+\frac{p+1}{2}; 1 \right] = \sum_{s=0}^{\min(\lambda_l, n_r-p)} \frac{(-n)_s(-\lambda_l)_s(-n_r+p)_s}{\left[-n_r+\frac{p}{2}\right]_s \left[-n_r+\frac{p+1}{2}\right]_s} \frac{1}{s!} , \tag{3.18a}$$

$$\begin{aligned} &{}_3F_2 \left[\frac{-\kappa_\sigma}{2}, -\frac{\kappa_\sigma-1}{2}, 1-i\gamma_1; \kappa+l+1, -p_\sigma-l; \frac{\Delta^2+Q^2}{\Delta^2} \right] \\ &\qquad = \sum_{u=0}^{[\kappa_\sigma/2]} \frac{(-\kappa_\sigma/2)_u(-\kappa_\sigma/2+1/2)_u(1-i\gamma_1)_u}{(\kappa+l+1)_u(-p_\sigma-l)_u u!} \left[\frac{\Delta^2+Q^2}{\Delta^2} \right]^u , \end{aligned} \tag{3.18b}$$

where $[\kappa_\sigma/2]$ is the integral part of the fraction $\kappa_\sigma/2$.

Thus far, the quantization axis has been kept arbitrary in the derivation of the general result (3.14). However, the angular momentum algebra can considerably be simplified by choosing the quantization axis along the incident velocity vector **v**. Such a choice is adopted in the present paper, so that[35]

$$H_{n_i n_f;\sigma}^{(\nu_i,\nu_f)}(\boldsymbol{\alpha},\boldsymbol{\beta}) = \hat{H}_{n_i n_f;\sigma}^{(\nu_i,\nu_f)}(\boldsymbol{\alpha}\cdot\mathbf{v},\boldsymbol{\beta}\cdot\mathbf{v}) \Phi_{m^f}^*(\phi_\alpha)\Phi_{m^i}(\phi_\beta) , \tag{3.19}$$

with $\hat{H}$ being independent of azimuthal angles ϕ_α and ϕ_β,

$$\begin{aligned} &(2/\pi)^{1/2} \hat{H}_{n_i n_f;\sigma}^{(\nu_i,\nu_f)}(\boldsymbol{\alpha}\cdot\mathbf{v},\boldsymbol{\beta}\cdot\mathbf{v}) \\ &\quad = \frac{1}{n_i! n_f!} \sum_{l_1^i=|m^i|}^{l^i} \sum_{l_1^f=|m^f|}^{l^f} \sum_{l=l^{if}}^{\lambda}{}^{(2)} (-1)^{(\lambda+l)/2-m^i} \frac{(2n_r!)}{n_r!} \Omega_{l_1^i l_1^f}^{lm}(v) \\ &\qquad\qquad \times \sum_{p=0}^{n_r} \frac{(-n_r)_p}{(-2n_r)_p} {}_3F_2 \left[-n, -\lambda_l, -n_r+p; -n_r+\frac{p}{2}, -n_r+\frac{p+1}{2}; 1 \right] \\ &\qquad\qquad \times \frac{2^{p-2n_r}}{p!} \int_0^1 dt\, t^{n_f+l_2^i}(1-t)^{n_i+l_2^f} \frac{g_{\bar{p}lm}^{(\sigma,\Delta)}(\mathbf{Q}\cdot\mathbf{v})}{\Delta^{2n-(\lambda+l)-p-1}} , \end{aligned} \tag{3.20}$$

where $m = m^i - m^f$,

$$\Omega^{lm}_{l_1^i l_1^f}(v) = (l_1^i \mid l^i m^i)(l_1^f \mid l^f m^f)\langle l_1^i m^i \mid l_1^f m^f \mid lm \rangle v^{l_2^f}(-v)^{l_2^i} , \tag{3.21a}$$

$$g^{(\sigma,\Delta)}_{\bar{p}lm}(\mathbf{Q}\cdot\mathbf{v}) = \sum_{\kappa=0}^{p_\sigma} \sum_{l_1=|m|}^{l} \mathcal{J}^{\kappa l_1}_{pl}(\sigma)\hat{D}^{\,l_1}_{lm}(\mathbf{Q}\cdot\mathbf{v}) , \tag{3.21b}$$

$$\hat{D}^{\,l_1}_{lm}(\mathbf{Q}\cdot\mathbf{v}) = (l_1 \mid lm)(-iv)^{l_2} Q^{l_1} \mathcal{P}_{l_1 m}(\hat{\mathbf{Q}}\cdot\hat{\mathbf{v}}) , \tag{3.21c}$$

and

$$(l_1^j \mid l^j m^j) = \left[\frac{2l^j+1}{2l_1^j+1} \frac{(l^j+m^j)!}{(l_1^j+m^j)!l_2^j!} \frac{(l^j-m^j)!}{(l_1^j-m^j)!l_2^j!} \right]^{1/2} \quad (j=i,f) , \tag{3.22a}$$

$$(l_1 \mid lm) = \left[\frac{2l+1}{2l_1+1} \frac{(l+m)!}{(l_1+m)!l_2!} \frac{(l-m)!}{(l_1-m)!l_2!} \right]^{1/2} \quad (m = m^i - m^f) , \tag{3.22b}$$

where $\mathcal{P}_{l_1 m}(z)$ is the normalized associated Legendre function of the first kind, i.e.,

$$\mathcal{P}_{l_1 m}(z) = (-1)^m \left[\frac{2l_1+1}{2} \frac{(l_1-m)!}{(l_1+m)!} \right]^{1/2} (1-z^2)^{m/2} \times \left[\frac{d}{dz} \right]^{l_1+m} \frac{(z^2-1)^{l_1}}{2^{l_1} l_1!} (m \geq 0) , \tag{3.23a}$$

$$\mathcal{P}_{l_1,-m}(z) = (-1)^m \mathcal{P}_{l_1 m}(z) , \tag{3.23b}$$

$$\Phi_m(\phi) = (2\pi)^{-1/2}\exp(im\phi) , \tag{3.23c}$$

$$\phi_\alpha = \phi_\eta, \quad \phi_\beta = \phi_\alpha + \pi . \tag{3.23d}$$

This completes the calculation of the transition amplitude for process (2.1) in the most general case of arbitrary initial and final quantum numbers i and f. Total cross section (2.15c) is obtained by carrying out the double integration over t and η with the quantization axis along vector $\mathbf{v}$. The integral over ϕ_η is performed analytically with the result equal to 2π. This is immediately apparent from Eq. (3.19). In practice, a change of variable is made in the integral over η, such as

$$z = (\eta^2-2)/(\eta^2+2) , \tag{3.24a}$$

which scales the integrand towards the dominant region of the narrow forward cone. This is more obvious if we rewrite Eq. (3.24a) in the following form:

$$\cos\theta = 1 - \left[\frac{1}{\mu_r v} \right]^2 \frac{1+z}{1-z} , \tag{3.24b}$$

where $\eta = 2\mu_r v \sin(\theta/2)$, θ is the scattering angle $\theta = \cos^{-1}(\hat{\mathbf{k}}_i \cdot \hat{\mathbf{k}}_f)$, and μ_r is the reduced mass of the incident and target nucleus. We choose the universal Gauss-Legendre quadrature to carry out both of the remaining integrals over $t \in [0,1]$ and $z \in [-1,-1]$. A variable order version of this integration rule is used to compute σ_{if} with any prescribed degree of accuracy. If necessary, the original integration domains are split into a number of segments in order to achieve the required precision of the total cross section. The numerical results reported in the present paper are exact to within three significant digits.

We have written a program for both reactions (2.1) and (2.7), which exactly reproduces the numerical results obtained by partial differentiation for all possible transitions between $n^i l^i m^i$ and $n^f l^f m^f$ with $n^i, n^f \leq 3$ and $0 \leq l^{i,f} \leq n^{i,f} - 1$, $-l^{i,f} \leq m^{i,f} \leq +l^{i,f}$. Further, a driving subroutine was written in order to detect numerical instabilities due to round-off error which can occur in alternating series for large quantum number values. If these series are found to cause a serious loss of significant digits, an efficient Shank-Levin nonlinear transformation is used to carry out the summations exactly.[41,42]

The two different branches of the present algorithm for reactions (2.1) and (2.7) can also intrinsically be tested against each other. The hydrogenlike wave function $\varphi_i^{Z_T}(\mathbf{r}_T)$ for the target in process (2.7) can easily be expressed as a linear combination of normalized STO's. Hence, in a number of test runs, for various combinations of initial and final states with appropriate specification of parameters, we have obtained the results of Belkić *et al.*[36] for process (2.7) by utilizing the path of the program devoted to reaction (2.1).

IV. RESULTS

We have presently computed the total cross sections for electron capture by protons from the K shell of He(^1S), N(^4S), and O(^3P), i.e.,

$$H^+ + \mathrm{He}(1s^2) \rightarrow H(n^f l^f m^f) + \mathrm{He}^+ , \tag{4.1a}$$

$$H^+ + \mathrm{N}(1s^2 2s^2 2p^3) \rightarrow H(n^f l^f m^f) + \mathrm{N}^+ , \tag{4.1b}$$

$$H^+ + \mathrm{O}(1s^2 2s^2 2p^4) \rightarrow H(n^f l^f m^f) + \mathrm{O}^+ , \tag{4.1c}$$

and

$$H^+ + \mathrm{He}(1s^2) \rightarrow H(\Sigma) + \mathrm{He}^+ , \tag{4.2a}$$

$$H^+ + \mathrm{N}(1s^2 2s^2 2p^3) \rightarrow H(\Sigma) + \mathrm{N}^+ , \tag{4.2b}$$

$$H^+ + \mathrm{O}(1s^2 2s^2 2p^4) \rightarrow H(\Sigma) + \mathrm{O}^+ . \tag{4.2c}$$

The model of Sec. II is adopted for these reactions with the RHF wave functions given by Clementi and Roetti.[38] For He (^1S),

$$\varphi_i^{\mathrm{RHF}}(\mathbf{r}_T)= 0.768\,38\chi_{100}^{(1.417\,14)}(\mathbf{r}_T)+0.223\,46\chi_{100}^{(2.376\,82)}(\mathbf{r}_T)+0.040\,82\chi_{100}^{(4.396\,28)}(\mathbf{r}_T)$$
$$-0.009\,94\chi_{100}^{(6.526\,99)}(\mathbf{r}_T)+0.002\,30\chi_{100}^{(7.942\,52)}(\mathbf{r}_T)\quad (E_i^{\mathrm{RHF}}=-0.917\,95,\ Z_T^{\mathrm{eff}}=1.354\,954)\ ; \tag{4.3a}$$

for N(^4S),

$$\varphi_i^{\mathrm{RHF}}(\mathbf{r}_T)= 0.937\,80\chi_{100}^{(6.457\,39)}(\mathbf{r}_T)+0.058\,49\chi_{100}^{(11.172\,00)}(\mathbf{r}_T)+0.000\,93\chi_{200}^{(1.364\,05)}(\mathbf{r}_T)$$
$$-0.001\,70\chi_{200}^{(1.897\,34)}(\mathbf{r}_T)+0.005\,74\chi_{200}^{(3.252\,91)}(\mathbf{r}_T)+0.009\,57\chi_{200}^{(5.082\,38)}(\mathbf{r}_T)$$
$$(E_i^{\mathrm{RHF}}=-15.629\,09,\ Z_T^{\mathrm{eff}}=5.590\,92)\ ; \tag{4.3b}$$

for O(^3P),

$$\varphi_i^{\mathrm{RHF}}(\mathbf{r}_T)= 0.945\,16\chi_{100}^{(7.614\,13)}(\mathbf{r}_T)+0.033\,91\chi_{100}^{(13.757\,40)}(\mathbf{r}_T)-0.000\,34\chi_{200}^{(1.698\,24)}(\mathbf{r}_T)$$
$$+0.002\,41\chi_{200}^{(2.480\,22)}(\mathbf{r}_T)-0.004\,86\chi_{200}^{(4.311\,96)}(\mathbf{r}_T)+0.036\,81\chi_{200}^{(5.865\,96)}(\mathbf{r}_T)$$
$$(E_i^{\mathrm{RHF}}=-20.668\,66,\ Z_T^{\mathrm{eff}}=6.429\,411)\ , \tag{4.3c}$$

where the values of effective nuclear charge Z_T^{eff} are obtained from Eq. (2.11).

We have also thoroughly investigated the hydrogenlike wave functions for the target atoms. Detailed computations based upon Eq. (2.1a) have presently been carried out by setting $Z_T=Z_T^{\mathrm{eff}}$ and choosing the same value for Z_T^{eff} as in the aforementioned RHF model, i.e., $Z_T^{\mathrm{eff}}=1.354\,954$, 5.590 92, and 6.429 411 for helium, nitrogen, and oxygen target atoms, respectively. The present first Born approximation involving the hydrogenic model is also consistently devised so that the correct boundary conditions are preserved. This is in contrast to the customary computations.[24–26,31]

The cross sections for capture into individual state of H($n^f l^f m^f$) for reactions (4.1) and (4.2) are displayed in Tables I–III. Contribution from the ground state of $H(1s)$ dominates the transitions of the electron into higher levels of atomic hydrogen for the processes under study. Hence, the present results for any final state of atomic hydrogen $H(\Sigma)$, which are produced in reactions (4.2a)–(4.2c), can be obtained with sufficient accuracy from the following simple expression with the spectroscopic notation for the cross sections:

$$\sigma_{\mathrm{total}}=\sigma_{1s}+1.616(\sigma_{2s}+\sigma_{2p})\ . \tag{4.4}$$

Here $\sigma_{if}=\sigma_f$, where index i is held fixed with reference to the K shell of He, N, and O. In a test run, capture into higher states of H($n^f l^f m^f$), with $n^f \geq 3$, is found to be negligible at all the impact energies covered (50 keV $\leq E \leq$ 50 MeV).

Comparison between the theory and experiments is depicted in Figs. 1–3. The RHF model for H^+-He collisions describes the measurements remarkably well at impact energies ranging from 50 keV to 10.5 MeV (see Fig. 1). Concerning H^+-N and H^+-O scatterings, only the experimental data of Cocke *et al.*[8] correspond to capture from the K shell of the target. Earlier measurements[1–5] did not isolate either of the K or L shell of nitrogen and oxygen. However, at high energies, the contribution from the K shell becomes dominant over that from the L shell.[6,35] Hence, we are justified, at least at higher energies, in displaying the findings of Acerbi *et al.*,[1] Schryber,[2] Welsh *et al.*,[3] Toburen *et al.*,[4] and Berkner *et al.*[5] in Figs. 2 and 3, together with the pure K-shell cross sections of Cocke *et al.*[8] Furthermore, in all the experiments quoted in Figs. 2 and 3, capture has been recorded from molecular targets N_2 and O_2. At high energies, it is customary to assume that scattering of molecular nitrogen N_2 proceeds as if the target were built from two independent (isolated) N atoms (an analogous assumption also holds for O_2). This implies that the simple scaling of the type $\sigma_{\mathrm{N}}=0.5\sigma_{\mathrm{N}_2}$ can be used to arrive at the experimental cross sections per gas atom (see Ref. 50 for limitations of the scaling). These are plotted in Figs. 2 and 3. Given these limitations, overall good agreement is obtained between the present RHF theory and the measurements. Of particular importance for high-energy theories is the measurement of Acerbi *et al.*[1] on charge exchange in H^+-N_2 and H^+-O_2 collisions performed at 32.5 and 37.7 MeV. It can be seen from Figs. 2 and 3 that our RHF model is very satisfactory even for these extremely fast projectiles.

Hydrogenlike and RHF wave functions of the target atom yield noticeably different results for the cross sections computed within the present CB1 approximation. At intermediate energies, the results obtained with the hydrogenic wave function are slightly larger than those due to the RHF orbitals for the target. The situation is reversed, however, at high energies, where the hydrogenic cross sections always lie considerably below the corresponding RHF results. In comparison with the experimental data in Figs. 1–3, it is observed that the RHF model represents a substantial improvement over the crude hydrogenlike wave function for the target atom.

V. CONCLUSIONS

It is very important to consistently design a first-order perturbation theory for charge exchange starting from the basic principles of atomic scattering. Here, "consistent" implies that the unperturbed channel states and the perturbing potentials are determined in accordance with the Coulomb boundary conditions for two charged

TABLE I. Total cross sections (in units of cm^2) for electron capture by H$^+$ from He(1s^2) as a function of laboratory impact energy E (keV). The rows labeled (a) and (b) refer to the Roothaan-Hartree-Fock (RHF) and the hydrogenic model for the target (see the text), respectively. In both of these models for the process under study, the correct boundary conditions are preserved in the entrance and exit channels. All the results are obtained by means of the corrected first Born (CB1) approximation (see the text). The present RHF model employs an arithmetic average [Eq. (2.13)] of the post and prior transition amplitudes and proceeds through Eqs. (2.2a) and (2.2b), (2.4a) and (2.4b), (2.9a) and (2.9b), (2.11), (2.14), (2.15c), and (2.16b). Similarly, the hydrogenic model is based upon Eqs. (2.8a), (2.8c), (2.11), and (2.14), where $T_{if}(\eta)$ is taken to be $T^{-}_{if}(\eta)$ (there is no post-priori discrepancy in our hydrogenic model). The row denoted by $2p$ refers to σ_{2p}, which is given by the usual relation of the type $\sigma_{2p}=\sigma_{210}+2\sigma_{211}$. The row labeled "Total" represents the cross section summed over all the bound states of H($n^f l^f m^f$) atom by virtue of Eq. (4.4), i.e., $\sigma_{\text{Total}}=\sigma_{1s}+1.616(\sigma_{2s}+\sigma_{2p})$. Notation $X[-N]$ implies $X\times10^{-N}$.

$n^f l^f m^f$	E (keV)	20	30	35	50	75	100	125	250
100	(a)	3.87[−16]	2.28[−16]	1.80[−16]	9.67[−17]	4.11[−17]	2.02[−17]	1.10[−17]	1.15[−18]
	(b)	4.25[−16]	2.50[−16]	1.97[−16]	1.04[−16]	4.27[−17]	2.03[−17]	1.07[−17]	9.82[−19]
200	(a)	2.54[−17]	1.99[−17]	1.72[−17]	1.07[−17]	5.15[−18]	2.67[−18]	1.49[−18]	1.60[−19]
	(b)	2.56[−17]	2.08[−17]	1.80[−17]	1.14[−17]	5.38[−18]	2.72[−18]	1.48[−18]	1.40[−19]
210	(a)	1.60[−17]	1.04[−17]	8.72[−18]	5.21[−18]	2.28[−18]	1.06[−18]	5.27[−19]	3.51[−20]
	(b)	3.06[−17]	1.67[−17]	1.30[−17]	6.86[−18]	2.73[−18]	1.20[−18]	5.75[−19]	3.32[−20]
211	(a)	1.36[−18]	1.08[−18]	9.90[−19]	6.97[−19]	3.38[−19]	1.62[−19]	8.14[−20]	5.33[−21]
	(b)	1.71[−18]	1.20[−18]	1.09[−18]	7.70[−19]	3.73[−19]	1.76[−19]	8.61[−20]	4.91[−21]
$2p$	(a)	1.87[−17]	1.26[−17]	1.07[−17]	6.60[−18]	2.96[−18]	1.38[−18]	6.90[−19]	4.57[−20]
	(b)	3.40[−17]	1.91[−17]	1.52[−17]	8.40[−18]	3.48[−18]	1.56[−18]	7.47[−19]	4.30[−20]
Total	(a)	4.58[−16]	2.81[−16]	2.25[−16]	1.25[−16]	5.42[−17]	2.68[−17]	1.45[−17]	1.49[−18]
	(b)	5.21[−16]	3.14[−16]	2.50[−16]	1.36[−16]	5.70[−17]	2.72[−17]	1.43[−17]	1.28[−18]

$n^f l^f m^f$	E (keV)	500	750	1000	2500	5000	7500	10 500	12 500
100	(a)	7.40[−20]	1.23[−20]	3.18[−21]	3.15[−23]	7.42[−25]	7.69[−26]	1.13[−26]	4.17[−27]
	(b)	5.22[−20]	7.61[−21]	1.80[−21]	1.35[−23]	2.73[−25]	2.65[−26]	3.76[−27]	1.36[−27]
200	(a)	1.01[−20]	1.64[−21]	4.20[−22]	4.04[−24]	9.42[−26]	9.71[−27]	1.43[−27]	5.25[−28]
	(b)	7.25[−21]	1.03[−21]	2.41[−22]	1.74[−24]	3.47[−26]	3.35[−27]	4.74[−28]	1.71[−28]
210	(a)	1.20[−21]	1.33[−22]	2.58[−23]	1.00[−25]	1.18[−27]	8.09[−29]	8.50[−30]	2.62[−30]
	(b)	9.37[−22]	9.12[−23]	1.61[−23]	4.70[−26]	4.67[−28]	3.01[−29]	3.03[−30]	9.18[−31]
211	(a)	1.74[−22]	1.87[−23]	3.56[−24]	1.29[−26]	1.43[−28]	9.56[−30]	9.87[−31]	3.02[−31]
	(b)	1.30[−22]	1.22[−23]	2.09[−24]	5.69[−27]	5.43[−29]	3.43[−30]	3.41[−31]	1.03[−31]
$2p$	(a)	1.55[−21]	1.70[−22]	3.29[−23]	1.26[−25]	1.46[−27]	9.999[−29]	1.05[−29]	3.23[−30]
	(b)	1.20[−21]	1.16[−22]	2.03[−23]	5.84[−26]	5.76[−28]	3.69[−29]	3.71[−30]	1.12[−30]
Total	(a)	9.28[−20]	1.52[−20]	3.91[−21]	3.82[−23]	8.97[−25]	9.27[−26]	1.37[−26]	5.03[−27]
	(b)	6.59[−20]	9.47[−21]	2.22[−21]	1.64[−23]	3.30[−25]	3.20[−26]	4.54[−27]	1.64[−27]

TABLE II. The same as in Table I except that capture is taking place from the K shell of N($1s^22s^22p^3$) by protons.

$n^fl^fm^f$ \ E (keV)		500	750	1000	2000	5000	10 000	20 000	50 000
100	(a)	5.53[−20]	2.90[−20]	1.60[−20]	2.35[−21]	7.19[−23]	2.93[−24]	8.55[−26]	5.75[−28]
	(b)	5.13[−20]	2.93[−20]	1.69[−20]	2.51[−21]	6.60[−23]	2.30[−24]	5.80[−26]	3.39[−28]
200	(a)	6.73[−21]	3.57[−21]	1.98[−21]	2.95[−22]	9.05[−24]	3.68[−25]	1.07[−26]	7.22[−29]
	(b)	6.08[−21]	3.56[−21]	2.08[−21]	3.15[−22]	8.32[−24]	2.89[−25]	7.28[−27]	4.24[−29]
210	(a)	1.27[−22]	7.38[−23]	4.17[−23]	5.37[−24]	9.41[−26]	2.12[−27]	3.21[−29]	8.73[−32]
	(b)	2.71[−22]	1.14[−22]	5.65[−23]	6.13[−24]	9.04[−26]	1.77[−27]	2.37[−29]	5.66[−32]
211	(a)	1.87[−23]	1.07[−23]	5.95[−24]	7.32[−25]	1.25[−26]	2.76[−28]	4.09[−30]	1.07[−32]
	(b)	1.98[−23]	1.09[−23]	6.50[−24]	8.57[−25]	1.25[−26]	2.34[−28]	2.97[−30]	6.71[−33]
$2p$	(a)	1.65[−22]	9.52[−23]	5.36[−23]	6.83[−24]	1.19[−25]	2.67[−27]	4.03[−29]	1.09[−31]
	(b)	3.10[−22]	1.36[−22]	6.95[−23]	7.85[−24]	1.15[−25]	2.24[−27]	2.96[−29]	7.00[−32]
Total	(a)	6.65[−20]	3.49[−20]	1.93[−20]	2.84[−21]	8.67[−23]	3.52[−24]	1.03[−25]	6.92[−28]
	(b)	6.16[−20]	3.53[−20]	2.04[−20]	3.03[−21]	7.96[−23]	2.77[−24]	6.98[−26]	4.07[−28]

TABLE III. The same as in Table I except that capture is taking place from the K shell of O($1s^22s^22p^4$) by protons.

$n^fl^fm^f$ \ E (keV)		500	750	1000	2500	5000	10 000	20 000	50 000
100	(a)	3.32[−20]	1.93[−20]	1.16[−20]	1.10[−21]	8.87[−23]	4.23[−24]	1.38[−25]	1.01[−27]
	(b)	2.73[−20]	1.79[−20]	1.16[−20]	1.20[−21]	8.76[−23]	3.60[−24]	1.01[−25]	6.32[−28]
200	(a)	4.04[−21]	2.38[−21]	1.44[−21]	1.38[−22]	1.11[−23]	5.31[−25]	1.73[−26]	1.27[−28]
	(b)	3.23[−21]	2.16[−21]	1.42[−21]	1.50[−22]	1.10[−23]	4.52[−25]	1.26[−26]	7.91[−29]
210	(a)	6.37[−23]	3.75[−23]	2.29[−23]	1.93[−24]	1.08[−25]	2.99[−27]	5.14[−29]	1.53[−31]
	(b)	1.43[−22]	6.41[−23]	3.41[−23]	2.26[−24]	1.10[−25]	2.67[−27]	4.03[−29]	1.05[−31]
211	(a)	7.62[−24]	5.16[−24]	3.27[−24]	2.62[−25]	1.41[−26]	3.84[−28]	6.50[−30]	1.88[−32]
	(b)	1.05[−23]	5.04[−24]	3.29[−24]	3.14[−25]	1.55[−26]	3.59[−28]	5.15[−30]	1.27[−32]
$2p$	(a)	7.90[−23]	4.78[−23]	2.94[−23]	2.46[−24]	1.36[−25]	3.76[−27]	6.44[−29]	1.91[−31]
	(b)	1.64[−22]	7.42[−23]	4.06[−23]	2.89[−24]	1.42[−25]	3.38[−27]	5.06[−29]	1.30[−31]
Total	(a)	3.98[−20]	2.32[−20]	1.40[−20]	1.33[−21]	1.07[−22]	5.10[−24]	1.66[−25]	1.21[−27]
	(b)	3.27[−20]	2.15[−20]	1.40[−20]	1.44[−21]	1.06[−22]	4.33[−24]	1.21[−25]	7.60[−28]

aggregates which are widely separated (Dollard[51]). A theory of this kind would supply invaluable information about the role of direct channels in charge exchange. Systematic and exhaustive comparison with experimental data over large energy intervals could subsequently indicate the relative importance of the neglected intermediate channels.

We have dealt with this problem by strictly applying the concept of the convergent S matrix, which was devised for the first time by Dollard.[51] In this theory, the scattering matrix for two charged particles interacting via Coulomb forces can only be defined if the Møller wave operators are reformulated by inclusion of the logarithmic phase distortion. This redefinition has a complicated functional dependence which is virtually impossible to implement in realistic computations. Fortunately, Dollard[51] has shown that the use of distorting Møller wave operators is equivalent to introducing the Coulomb phase distortion of the unperturbed scattering states. This formalism can directly be extended to three-particle

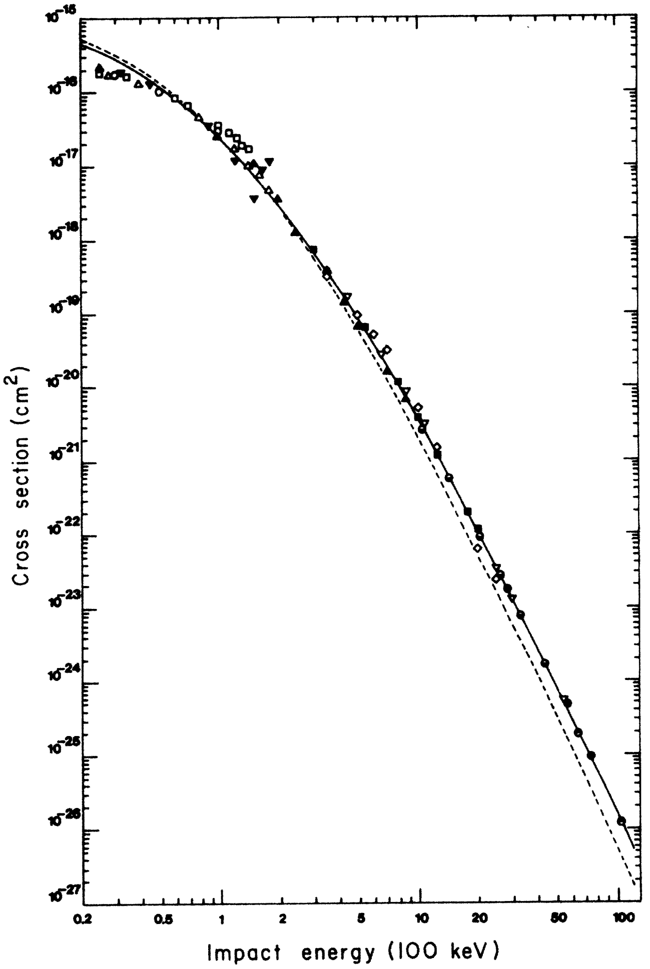

FIG. 1. Total cross sections for electron capture by H^+ from He($1s^2$). Present results: ——, the corrected first Born (CB1) approximation with the Roothaan-Hartree-Fock (RHF) model; — — —, the CB1 approximation with the hydrogenic model). In both models the correct boundary conditions are preserved in the entrance and exit channels (see the text). Experimental data: ◒, Schryber (Ref. 2); ∇, Welsh *et al.* (Ref. 3); ■, Toburen *et al.* (Ref. 4); ◓, Berkner *et al.* (Ref. 5); △, Stier and Barnett (Ref. 43); ▲, Barbett and Reynolds (Ref. 44); ▼, Afrosimov *et al.* (Ref. 45); □, de Heer *et al.* (Ref. 46); ◇, Williams (Ref. 47); ○, Martin *et al.* (Ref. 48); ●, Horsdal-Pedersen *et al.* (Ref. 49). Theoretical results σ_{Total} are obtained from the following equation: $\sigma_{\text{Total}}=\sigma_{1s}+1.616(\sigma_{2s}+\sigma_{2p})$. Inclusion of higher excited states of $H(n^f l^f m^f)$ does not change the theoretical curves on the shell given in this figure (see also Tables I). Measurements relate to process (4.2a) where the hydrogen atom is produced in any state.

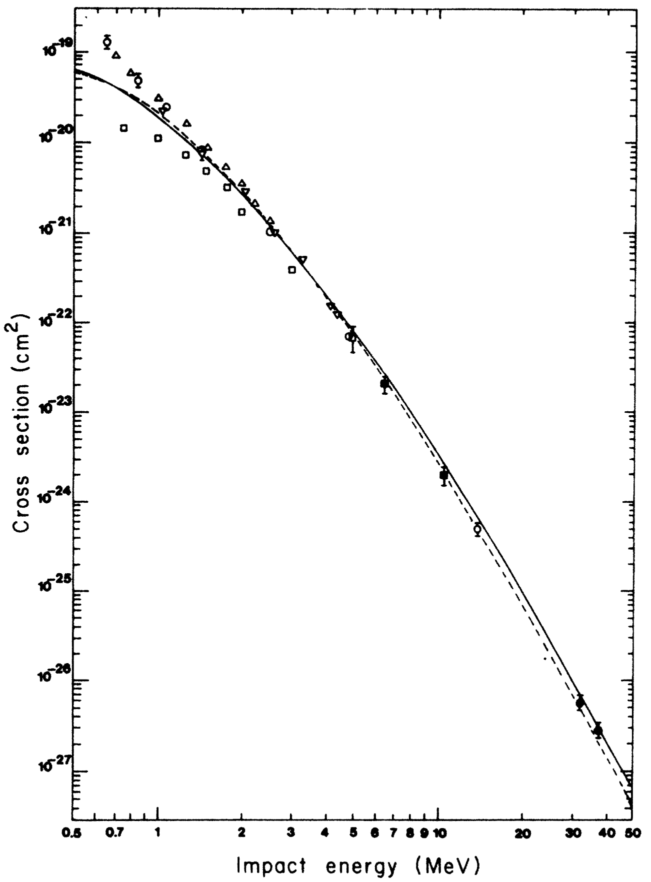

FIG. 2. Total cross sections for electron capture by H^+ from the K shell of N($1s^2 2s^2 2p^3$). Present results: ——, the corrected first Born (CB1) approximation with the Roothaan-Hartree-Fock (RHF) model; — — —, the CB1 approximation with the hydrogenic model. In both models the correct boundary conditions are preserved in the entrance and exit channels (see the text). Experimental data (all shells of nitrogen target): ●, Acerbi *et al.* (Ref. 1); △, Schryber (Ref. 2); ○, Welsh *et al.* (Ref. 3); △, Toburen *et al.* (Ref. 4); ■, Berkner *et al.* (Ref. 5). Experimental data (K shell of nitrogen target): □ Cocke *et al.* (Ref. 8). Original measurements (Refs. 1–5, 8) have been carried out on molecular nitrogen N_2 as target. Data per gas atom are plotted (σ_N). These are deduced from the observed findings (σ_{N_2}) by the following simple scaling: $\sigma_N=0.5\sigma_{N_2}$. Theoretical results σ_{Total} are obtained from the equation $\sigma_{\text{Total}}=\sigma_{1s}+1.616(\sigma_{2s}+\sigma_{2p})$. Inclusion of higher excited states of $H(n^f l^f m^f)$ does not change the theoretical curves on the shell given in this figure (see also Table II). Measurements correspond to reaction (4.2b) with the hydrogen atom H(Σ) left in any final states.

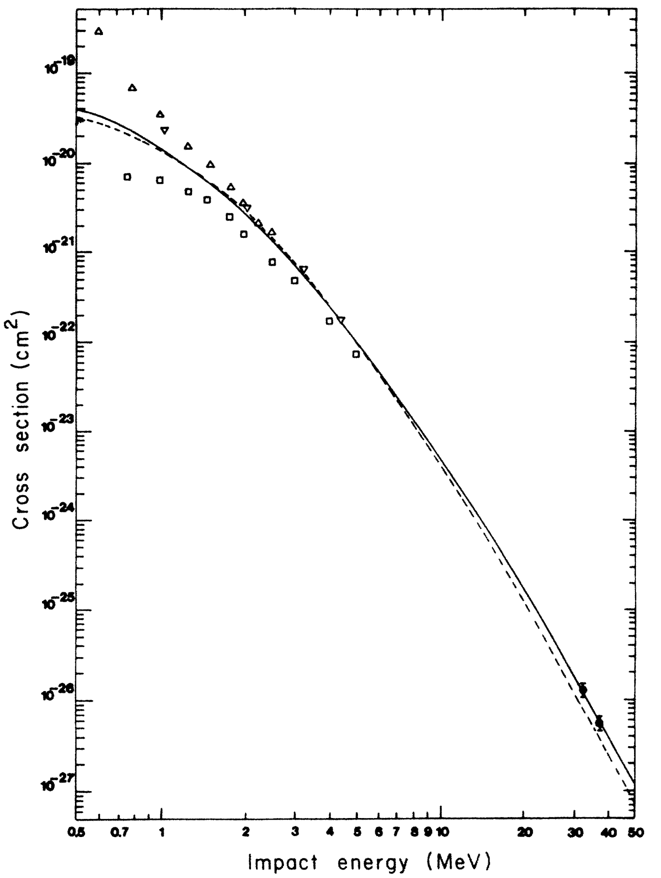

FIG. 3. Total cross sections for electron capture by H^+ from the K shell of $O(1s^2 2s^2 2p^4)$. Present results: ——, the corrected first Born (CB1) approximation with the Roothaan-Hartree-Fock (RHF) model; — — —, the CB1 approximation with the hydrogenic model. In both models the correct boundary conditions are preserved in the entrance and exit channels (see the text). Experimental data (all shells of oxygen target): ●, Acerbi *et al.* (Ref. 1); ∇, Schryber (Ref. 2); △, Toburen *et al.* (Ref. 4). Experimental data (K shell of oxygen target): □, Cocke *et al.* (Ref. 8). Original measurements (Refs. 1, 2, 4, and 8) have been performed on molecular oxygen O_2 as target. We have displayed converted data σ_O per gas atom which are related to the measured values σ_{O_2} by the expression $\sigma_O = 0.5\sigma_{O_2}$. Theoretical results σ_{Total} are obtained from the equation $\sigma_{\text{Total}} = \sigma_{1s} + 1.616(\sigma_{2s} + \sigma_{2p})$. Inclusion of higher excited states of $H(n^f l^f m^f)$ does not change the theoretical curves on the shell given in this figure (see also Table III). Measurements correspond to process (4.2c) where the hydrogen atom is produced in any final state $H(\Sigma)$.

collisions by identifying a pair of charged aggregates whose total interaction exhibits an asymptotic Coulomb tail. In this way, Belkić *et al.*[6] have obtained an exact and consistent eikonal T matrix for charge exchange, which is free of the characteristic Coulomb divergencies.[52] We presently utilize the first order of this theory, which is referred to as the corrected first Born (CB1) approximation. The corrections are such that the usual full first Born method of the Jackson-Schiff–type is reformulated by imposing the asymptotically exact boundary conditions to the scattering wave functions and the perturbation potentials.

Detailed comparison is carried out between the CB1 approximation and experiments on electron capture by protons from the K shell of helium, nitrogen, and oxygen in a very large range of the impact energy. It is found that the present Roothaan-Hartree-Fock (RHF) model, which is introduced within the CB1 theory, yields excellent agreement with the measurements. This is observed at incident proton energies $E\ (\text{keV}) \geq 60\,|E_i^{\text{RFH}}|$, where E_i^{RHF} is the RHF orbital energy of the captured electron. It is concluded that the CB1 method is highly reliable for computation of total cross sections from intermediate to very high energies.

ACKNOWLEDGMENTS

This material is based on work supported by the U.S.-Yogoslav Joint Fund for Scientific and Technological Cooperation, under the auspices of National Science Foundation (NSF) Grant No. JFP-516. All the computations were carried out on an IBM 4381/41 at the Serbian State Institute of Statistics in Belgrade through the Computing Laboratory of the Faculty of Science, University of Belgrade, Yugoslavia.

APPENDIX

There is a number of misprints in Ref. 35 and they should be corrected as follows:

On page 1993, in Eq. (2.9), $(|\mathbf{q}-\boldsymbol{\alpha}|^2+\alpha_f^2)^{\nu_f}$ should read $(|\mathbf{q}-\boldsymbol{\alpha}|^2+a_f^2)^{\nu_f}$; in Eq. (2.10), $\boldsymbol{\alpha}+\boldsymbol{\beta}=\mathbf{v}$ should read $\boldsymbol{\alpha}+\boldsymbol{\beta}=-\mathbf{v}$; in Eq. (2.12), $(Z_K/n^j)^{p_j}$ should read $(Z_K/n^j)^{2p_j}$,

On page 1995, in Eq. (2.34), $\tilde{\mathcal{T}}_{nlm}^{(\sigma,\Delta)}(\mathbf{Q})$ should read $\tilde{\mathcal{T}}_{nlm}^{(\sigma,\Delta)}(\mathbf{Q})/2^{n-1}$.

On page 1996, in Eq. (2.43b), $(-k_\sigma+\frac{1}{2})_u$ should read $(-k_\sigma/2+\frac{1}{2})_u$; in Eq. (2.49), $\mathcal{P}_{l_1 m}(\mathbf{Q}\cdot\hat{\mathbf{v}})$ should read $\mathcal{P}_{l_1 m}(\hat{\mathbf{Q}}\cdot\hat{\mathbf{v}})$.

On page 1999, in Eq. (4.6d), the number multiplying cross section $\sigma_{i;4}^{(1)}$ should read 2.561 instead of 3.113.

On page 2000, in Table I(c), n should read n^f.

On page 2001, in Table II(c), n should read n^f. Also in the same table, there are two misprints at 250 and 500 keV. The last number which corresponds to $n^f=4$ at 250 keV should read 8.25[−18] instead of 2.25[−18]. The second number corresponding to $n^f=2$ at 500 keV should be 5.12[−19] instead of 5.17[−19].

On page 2002, in Table III, the column labeled K refers to the K-shell cross section which is multiplied by 2 in order to account for the two K-shell electrons. In Eq. (A9), $\tilde{\chi}_{\bar{p}lm}^{(\Delta)}(\mathbf{Q})$ should read $\chi_{\bar{p}lm}^{(\sigma,\Delta)}(\mathbf{Q})$.

On page 2003, in Eq. (A12), $(\kappa_\sigma-1)/2$ should read $-(\kappa_\sigma-1)/2$.

On page 2004, in Eq. (B8), $C_{p+\nu}^{l+1}(\omega_+/\tau_+^{1/2})$ should read $C_{p+\sigma}^{l+1}(\omega_+/\tau_+^{1/2})$.

On page 2005, on the top line, $N_{p_1\sigma}^{pl}=N_{\bar{p}l}^{\sigma}b_{p_1\sigma}^{pl}$, should read $N_{p_1\sigma}^{pl}=N_{pl}^{\sigma}b_{p_1\sigma}^{pl}$; in Eq. (B22), $(1+yz)^k$ should read $(1+yz)^{k'}$.

[1] E. Acerbi, M. Castiglioni, G. Dutto, F. Resmini, C. Succi, and G. Tagliaferri, Nuovo Cimento B **50**, 176 (1967).

[2] U. Shryber, Helv. Phys. Acta. **40**, 1023 (1967).

[3] L. M. Welsh, K. H. Berkner, S. N. Kaplan, and R. V. Pyle, Phys. Rev. **158**, 85 (1967).

[4] L. H. Toburen, M. Y. Nakai, and R. A. Langley, Phys. Rev. **171**, 114 (1968).

[5] K. H. Berkner, S. N. Kaplan, G. A. Paulikas, and R. V. Pyle, Phys. Rev. **140**, 729 (1965).

[6] Dž. Belkić, R. Gayet, and A. Salin, Phys. Rep. **56**, 279 (1979).

[7] J. R. Macdonald, C. L. Cocke, and W. W. Edison, Phys. Rev. Lett. **32**, 648 (1974).

[8] C. L. Cocke, R. K. Gardner, B. Curnutte, T. Bratton, and T. K. Saylor, Phys. Rev. A **16**, 2248 (1977).

[9] M. Rødbro, E. Horsdal-Pedersen, C. L. Cocke, and J. R. Macdonald, Phys. Rev. A **19**, 1936 (1979).

[10] E. Horsdal-Pedersen, C. L. Cocke, J. L. Rasmussen, C. L. Varghese, and W. Waggoner, J. Phys. B **16**, 1799 (1983).

[11] S. Andriamonje, J. F. Chemin, J. Roturier, J. N. Scheurer, H. Laurent, and J. P. Schapira, in *Abstracts of Contributed Papers, Twelfth International Conference on the Physics of Electronic and Atomic Collisions, Gatlinburg, 1981,* edited by S. Datz (North-Holland, Amsterdam, 1981), p. 657.

[12] A. M. Halpern and J. Law, Phys. Rev. Lett. **31**, 4 (1973).

[13] J. R. Macdonald, L. M. Winters, M. D. Brown, L. D. Ellsworth, T. Chiao, and E. W. Pettus, Phys. Rev. Lett. **30**, 251 (1973); L. M. Winters, J. R. Macdonald, M. D. Brown, T. Chiao, L. D. Ellsworth, and E. W. Pettus, Phys. Rev. A **8**, 1835 (1973); J. R. Macdonald, M. D. Brown, S. J. Czuchlewski, L. M. Winters, R. Laubert, I. A. Sellin, and J. R. Mowat, Phys. Rev. A **14**, 1997 (1976).

[14] F. Hopkins, N. Cue, and V. Dutkiewitz, Phys. Rev. A **12**, 1710 (1975); F. Hopkins, R. Brenn, A. R. Whittmore, N. Cue, V. Dutkiewitz, and R. P. Chaturvedi, *ibid.* **13**, 74 (1976).

[15] C. W. Woods, R. L. Kauffman, K. A. Jamison, C. L. Cocke, and P. Richard, J. Phys. B **7**, L474 (1974); C. W. Woods, R. L. Kauffman, K. A. Jamison, N. Stolterfort, and P. Richard, Phys. Rev. A **13**, 1358 (1976).

[16] T. J. Gray, P. Richard, K. A. Jamison, J. M. Hall, and R. K. Gardner, Phys. Rev. A **14**, 1333 (1976); R. K. Gardner, T. J. Gray, P. Richard, C. Shmiedekamp, K. A. Jamison, and J. M. Hall, *ibid.* **15**, 2202 (1977).

[17] J. H. McGuire, Phys. Rev. A **8**, 2760 (1973).

[18] J. T. Hogan and H. C. Howe, J. Nucl. Mater. **63**, 151 (1976).

[19] R. E. Olson and A. S. Schlachter, Comments At. Mol. Phys. **18**, 237 (1986); Princeton Plasma Physics Laboratory Report No. PPPL-1327, 1976 (unpublished).

[20] H. W. Drawin, Phys. Rep. **37**, 125 (1978).

[21] H. B. Gilbody, Adv. At. Mol. Phys. **15**, 293 (1979); *Invited Papers of the Twelfth International Conference on the Physics of Electronic and Atomic Collisions, Gatlinburg, 1981,* edited by S. Datz (North-Holland, Amsterdam, 1981), p. 223.

[22] J. Silk and G. Steigman, Phys. Rev. Lett. **23**, 597 (1969).

[23] W. D. Watson, Astrophys. J. **206**, 842 (1975).

[24] C. D. Lin, S. C. Soong, and L. N. Tunnell, Phys. Rev. A **17**, 1646 (1978).

[25] L. Kocbach, J. Phys. B **13**, L665 (1980).

[26] T. S. Ho, M. Lieber, F. T. Chan, and K. Omidvar, Phys. Rev. A **24**, 2933 (1981).

[27] G. C. Saha, S. Datta, and S. C. Mukherjee, Phys. Rev. **31**, 3633 (1985).

[28] I. M. Cheshire, Proc. Phys. Soc. London **82**, 113 (1963); **84**, 89 (1964); D. R. Bates, Proc. R. Soc. London, Ser. A **247**, 294 (1958); G. C. Saha, S. Data, and S. C. Mukherjee, Phys. Rev. **34**, 2809 (1986).

[29] J. S. Briggs, Rep. Prog. Phys. **39**, 217 (1976).

[30] J. H. McGuire and L. Weaver, Phys. Rev. A **16**, 41 (1977).

[31] K. Omidvar, J. E. Golden, J. H. McGuire, and L. Weaver, Phys. Rev. A **13**, 500 (1976).

[32] J. H. McGuire, J. Phys. B **18**, L75 (1985).

[33] Dž. Belkić, R. Gayet, J. Hanssen, and A. Salin, J. Phys. B **19**, 2945 (1986).

[34] Dž. Belkić, S. Saini, and H. S. Taylor, Z. Phys. D **3**, 59 (1986).

[35] Dž. Belkić and H. S. Taylor, Phys. Rev. A **35**, 1991 (1987).

[36] Dž. Belkić, S. Saini, and H. S. Taylor, Phys. Rev. A **36**, 1601 (1987).

[37] D. P. Dewangan and J. Eichler, J. Phys. B **19**, 2939 (1986).

[38] E. Clementi and C. Roetti, At. Data Nucl. Data Tables **14**, 177 (1974).

[39] Dž. Belkić, J. Phys. B **17**, 3629 (1984).

[40] M. Abramowitz and I. Stegun, *Handbook of Mathematical Functions with Formulas, Graphs and Mathematical Tables* (Dover, New York, 1982).

[41] T. Fessler, W. F. Ford, and D. A. Smith, ACM Trans. Math. Software **9**, 346 (1983).

[42] Dž. Belkić, Phys. Rev. A (to be published).

[43] P. M. Stier and C. F. Barnett, Phys. Rev. **103**, 896 (1956).

[44] C. F. Barnett and H. K. Reynolds, Phys. Rev. **109**, 355 (1958).

[45] V. V. Afrosimov, R. N. Il'in, and E. S. Solov'ev, Zh. Tekhn. Fiz. **30**, 705 (1960) [Sov. Phys.—Techn. Phys. **5**, 661 (1960)].

[46] F. J. de Heer, J. Van Eck, and J. Kistemaker, *Proceedings of the Sixth International Conference on Ionization Phenomena in Gases, Paris, 1963,* edited by P. Hubert (SERMA, Paris, 1964), Vol. I, p. 73.

[47] J. F. Williams, Phys. Rev. **157**, 97 (1967).

[48] P. J. Martin, K. Arnett, D. M. Blankeship, T. J. Kvale, J. L. Peacher, E. Redd, V. C. Sutcliffe, J. T. Park, C. D. Lin, and J. H. McGuire, Phys. Rev. A **23**, 2858 (1981).

[49] E. Horsdal-Pedersen, C. L. Cocke, and M. Stockli, Phys. Rev. Lett. **50**, 1910 (1983).

[50] G. Ryding, A. B. Wittkower, and H. B. Gilbody, Proc. Phys. Soc. London **89**, 547 (1966); J. E. Bayfield, Phys. Rev. **185**, 115 (1969); A. B. Wittkower, G. Ryding, and H. B. Gilbody, Proc. Phys. Soc. London **171**, 89 (1966).

[51] D. Dollard, Ph.D. thesis, University of Michigan, 1963; J. Math. Phys. **5**, 729 (1964).

[52] R. A. Mapleton, Proc. Phys. Soc. London, **91**, 868 (1967); C. P. Carpenter and T. F. Tuan, Phys. Rev. A **2**, 1811 (1970); D. P. Dewangan and J. Eichler, J. Phys. B **18**, L65 (1985).